

Thermal stability of Li-rich cathode under long-duration

47-206113 Haochong Zhao, Supervisor: Prof. Yoshihisa Harada

1. Introduction and Significance

Lithium-ion batteries (LiBs) have been widely used in our daily life. However, thermal runaway of high energy density LiBs has caused many incidents in electric vehicles. Therefore it is necessary to investigate the thermal stability of cathode and anode in LiBs. Li-rich cathode, $\text{Li}_{1+x}\text{Ni}_y\text{Co}_z\text{Mn}_{(1-x-y-z)}\text{O}_2$, is a potential next-generation cathode material with a higher energy density than the conventional layered cathodes. Many studies have been focused on its voltage fade and O_2 release under long-duration. There are few studies on its thermal behavior, especially under long-duration. As a result, it is necessary to investigate the thermal degradation mechanism.

At present, there is a lack of connection between the surface structure and thermal stability of Li-rich cathode materials, especially under long-durations. Thus, the purpose of the present study is to investigate the element-specific mechanism of thermal decomposition behavior on Li-rich cathode under long-duration. Here, $\text{Li}_{1.2}\text{Ni}_{0.13}\text{Co}_{0.13}\text{Mn}_{0.54}$ was used as a typical Li-rich sample. Differential scanning calorimetry (DSC) measurements were carried out under 2nd, 50th and 200th cycles. DSC measurements can detect the heat flow of samples during the heating process. X-ray absorption spectroscopy (XAS) and resonant X-ray photoemission spectroscopy (RXPS) measurements were carried out for detailed thermal decomposition analysis.

2. Methods and Experiments

Electrochemical evaluation: The positive electrode consist of Li-rich materials, carbon black and PVDF with mass ration of 8:1:1. Li metal and commercialized electrolyte with perfluoroalkyl ethylene carbonate for high voltage were used. Li-rich materials with different cycles and charging to 4.8 V were prepared by coin cells (Cycling rate: 25mA/g for 1st and final cycles and 125mA/g for the other cycles).

DSC measurement: Cycled Li-rich cathodes were washed with dimethyl carbonate (DMC). DSC analysis was conducted from 25 °C to 600 °C at a scan rate of 10 K/min under argon flow.

XAS and RXPS measurements: O *K*-edge, Mn, Co, and Ni *L*-edges XAS spectra were measured by the surface-sensitive total-electron-yield (TEY) mode and the bulk-sensitive partial-fluorescence yield (PFY) mode at HORNET station of SPring-8 BL07LSU.

The probing depths of TEY and PFY are less than 10 nm and about 100 nm, respectively. RXPS for O, Ni, Co, and Mn valence bands were measured at 3DnanoESCA station of SPring-8 BL07LSU where the excitation energy was tuned to the energy of the characteristic peak in the XAS result obtained by the TEY mode.

3. Results and Discussion

Figure 1 shows the typical charge (solid) and discharge (dash dot) curves of Li-rich battery cells with 1st, 2nd, 50th, 100th and 200th cycles. The 1st charge curve shows two “plateaus”, which represent oxidation of transition metal (TM) and

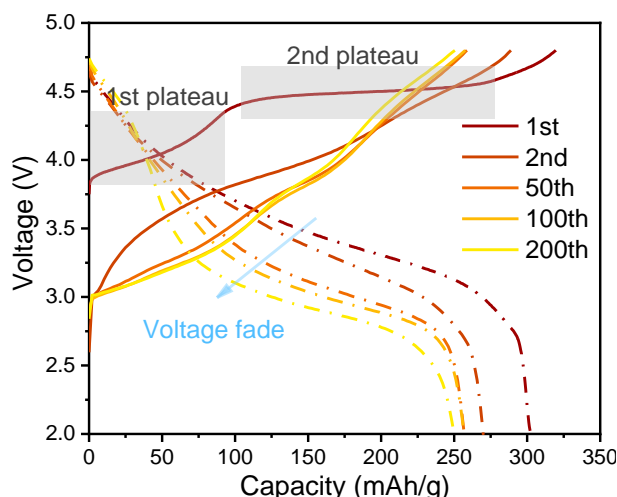


Figure 1. Charge (solid)-discharge (dash dot) curves for Li-rich battery cell with 1st, 2nd, 50th and 100th and 200th.

O²⁻, respectively [2]. However, in the 1st discharge, and the subsequent charge and discharge cycles, such “plateau” disappear and become monotonous. More importantly, there is a very significant voltage fade during cycling, especially between the 1st and 2nd cycles.

The voltage fade is mainly caused by the following two factors:

1. Decomposition of oxidized O species to O₂ and their releasing. [3]
2. The migration of TM ions will change the chemical environment and lead to a decrease of redox potential.[4]

With increasing the cycling numbers, the average valence states for Ni, Co and Mn are continuously reduced due to O₂ release. The reduction of TMs may increase the thermal stability of cathode because low-valence TMs are stable. On the other hand, O₂ release will form more oxygen vacancy and destroy the lattice structure, which may do harm to the thermal stability of cathode. Thermal decomposition of the Li-rich cathode at the first fully charged state undergoes phase transitions with O₂ release: layer phase → spinel phase → rock salt phase[5]. However, it is still difficult to predict the precise thermal stability of Li-rich materials under long-duration.

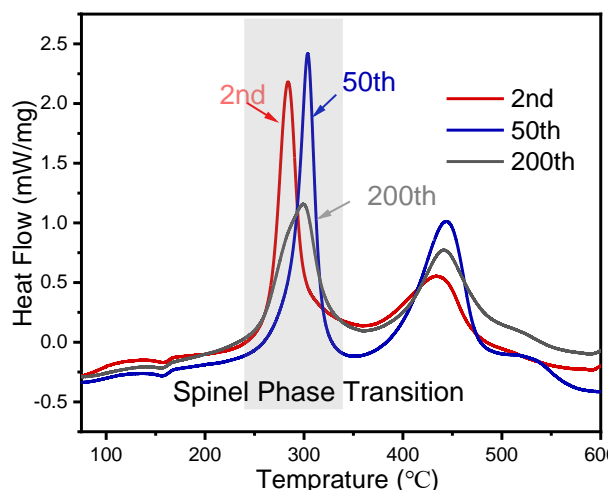


Figure 2. DSC result of 2nd(red), 50th(blue) and 200th(grey) cycles Li-rich cathode materials.

To investigate the thermal stability under long-duration, DSC measurements were performed. As shown in **Figure 2**, the first peak is related to layered → spinel phase transition. From 2nd to 50th cycles, the onset of the thermal decomposition temperature increased, which can be well explained by the reduction of Ni, Co and Mn during cycling according to the previous study [3]. However, 200th cycled samples show an interesting change: The degradation peak becomes wider and less intense, while the onset of the thermal decomposition temperature shows less change, or even decreased compared to the 50th cycled sample. It indicates that the reaction rate of the phase transition is slowed down kinetically.

To explain the mechanism of thermal behavior evolution under long-duration, XAS with TEY and PFY modes and RXPS measurements were performed to elucidate the electronic structure evolutions of charged Li-rich samples under different cycling.

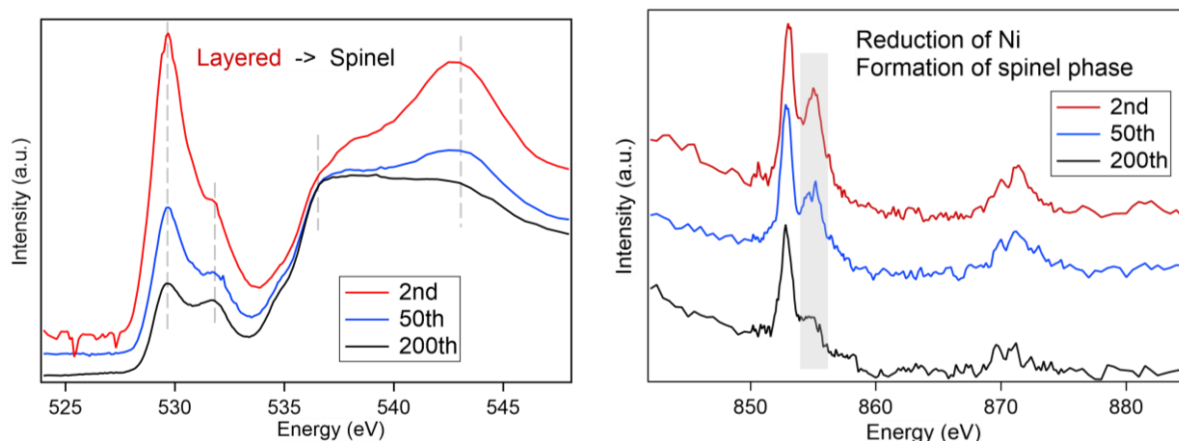


Figure 3. (a) O K-edge XAS, (b) Ni L-edge XAS. The results are collected in the TEY mode.

Figure 3 shows (a) O *K*-edge and (b) Ni *L*-edge XAS results obtained by the TEY mode. An obvious electronic structure change appeared for both O and Ni sites on the Li-rich cathode under long-duration. The other XAS and RXPS results will be discussed in the presentation. The O pre-edge peak after the 200th cycle is similar to that of the spinel LiM₂O₄ (M=Ni, Mn) cathode [6]. Meanwhile, the decrease of the peak intensity at 855 eV not only shows the reduction of Ni after cyclings but also related to the formation of the spinel phase.[6,7] The results indicate that the layered phase was transferred to the spinel phase at the surface area of the 200th cycled Li-rich cathode. The spinel phase usually has better thermal stability. Considering the phase transition and O₂ release occurring first at the surface of the cathode, the spinel phase formed at the surface area may inhibit the O₂ release kinetically. In the bulk area, it is still a layered structure with tiny reduction of TM due to tiny O₂ release during cycling, which can explain the increase on onset temperature. However, on the other hand, O₂ release will also cause accumulation of O vacancies, which do harm to lattice stability [7]. At 200th cycles, the influence of O vacancy is more than TM reduction and cause decrease on onset temperature. Other explanation will be shown in presentation. Accordingly, the XAS results have a good explanation on the change of thermal behavior under long-duration.

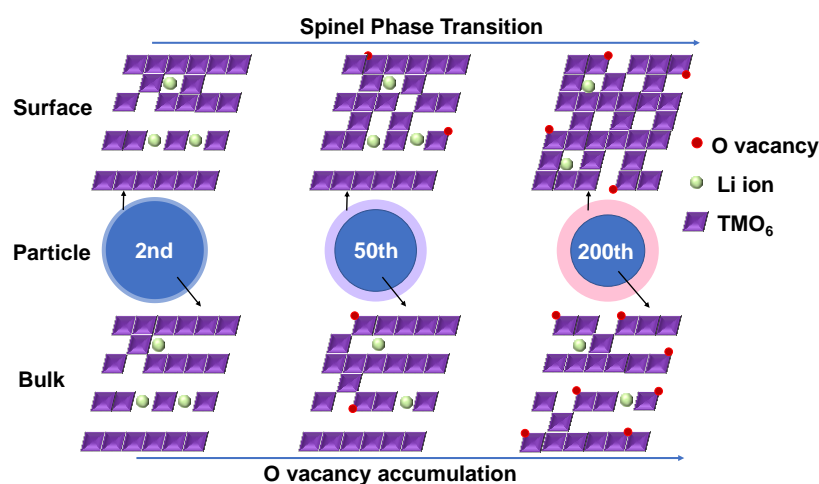


Figure 4. Schematic of structure evolution in surface and bulk area under long-duration

4. Summary

The electrochemical property shows the typical behavior of Li-rich cathode with obvious voltage fade during cycling. The thermal analysis of Li-rich cathode shows changes on thermal behavior. Especially at the 200th cycle, the phase transition from layered to spinel is kinetically suppressed. The tiny degradation temperature change under long duration can be explained by the reduction of TM and the increase of the O vacancies at the charged state.

However, the influence of TM migration in the bulk area under cycling was hard to probe by RXPS measurements, which may be related to the fine variations in thermal behavior. This problem will be the next challenge in the near future.

Acknowledgement

I'd like to express my deepest gratitude to Prof. Xiqian Yu at Institute of Physics Chinese Academy of Sciences for supporting my research during the period when I could not enter Japan due to the coronavirus pandemic.

Reference

- [1] J. Geder *et al.*, Solid State Ionics **268** (2014) 242–246. [2] H. Koga *et al.*, J. Phys. Chem. C **118** (2014) 5700–5709. [3] E. Hu *et al.*, Nat. Energy **3** (2018) 690–698. [4] R. A. House *et al.*, Nat. Energy **5** (2020) 777–785. [5] S. Muhammad *et al.*, J. Power Sources **285** (2015) 156–160. [6] H. Sun *et al.*, Adv. Funct. Mater. **32** (2022) 211279. [7] I. Takahashi, *et al.* J. Power Sources **401** (2018) 263–270. ACS Appl. Energy Mater. **2**(2019), 8188–8124.